

Signatures of the Sudden Stratospheric Warming events of January–February 2008 in Seoul, S. Korea

Evelyn De Wachter^{a,*}, Klemens Hocke^{a,c}, Thomas Flury^a, Dominik Scheiben^a,
Niklaus Kämpfer^{a,c}, Soohyun Ka^b, Jung Jin Oh^b

^a Institute of Applied Physics, University of Bern, Switzerland

^b Department of Chemistry, Sookmyung Women's University, Seoul, South Korea

^c Oeschger Centre for Climate Change Research, University of Bern, Switzerland

Received 9 August 2010; received in revised form 28 July 2011; accepted 3 August 2011

Available online 12 August 2011

Abstract

The period January–February 2008 was characterized by four Sudden Stratospheric Warmings (SSWs) in the Northern Hemisphere, of which the last warming, at the end of February 2008, was a major warming. A significant decrease in mesospheric water vapour (H₂O) of more than 2 ppmv (~40%) was observed by the ground-based microwave (GBMW) radiometer in Seoul, S. Korea [37.3°N, 126.3°E] during the major SSW. A comparison with ground-based mesospheric H₂O observations from the mid-latitude station in Bern [46.9°N, 7°E] revealed an anticorrelation in the mesospheric H₂O data during the major SSW. In addition, prior to the major warming, strong periodic fluctuations were recorded in the Aura MLS vertical temperature distribution between 15 and 0.05 hPa at Seoul. The mesospheric temperature oscillation was found to have a period of ~10–14 days with a persistency of 3–4 cycles.

The observed anticorrelation in mesospheric H₂O between the stations in Seoul and Bern is associated with an increased meridional flow. Trajectory calculations give evidence that H₂O-rich subtropical air had moved to Bern during the major SSW while H₂O-poor polar air was transported to Seoul.

The results shown in this study are a possible indication of a strong coupling between the dynamic regimes of the low- and the high-latitude regions during SSWs.

© 2011 COSPAR. Published by Elsevier Ltd. All rights reserved.

Keywords: Water vapour; Sudden Stratospheric Warming; Mesosphere; Planetary wave

1. Introduction

Sudden Stratospheric Warmings (SSWs) are characteristic winter phenomena mainly occurring in the Northern Hemisphere, where the high latitude stratospheric temperature rises abruptly by several tens of degrees, accompanied by a deceleration or reversal of the winter westerly (E-ward) jet, the latter being assigned as a major SSW. The widely accepted mechanism for SSWs is the vertical propagation of planetary waves (PWs), primarily zonal wave numbers 1 and 2, and their non-linear interaction

with the zonal mean flow, causing deceleration or reversal of the E-ward winds in the stratosphere and mesosphere. The deceleration of the westerly winds leads to downwelling and adiabatic heating of stratospheric air. Coincidental upwelling in the mesosphere induces a mesospheric cooling (Matsuno, 1971; Liu and Roble, 2002).

Clear signatures of mesospheric cooling during SSWs were reported by Walterscheid et al. (2000), Siskind and Coy (2005), and Hoffman et al. (2007). Citations following Siskind et al. (2010) explain that stratospheric wind shears during the SSW suppress the upward propagation of gravity waves into the mesosphere. The reduced breaking of mesospheric gravity waves leads to mesospheric cooling via a reduced wave-induced downwelling (Garcia et al., 1994). Hoffman et al. (2007) also found that the onset of the mesospheric cooling, accompanied by a reversal of

* Corresponding author. Address: Microwave department, Institute of Applied Physics, University of Bern, Sidlerstrasse 5, 3012 Bern, Switzerland. Tel.: +41 (0) 31 631 89 11; fax: +41 (0) 31 631 37 65.

E-mail address: dewachte@iap.unibe.ch (E. De Wachter).

the mesospheric circulation from E-ward to W-ward winds during the major SSW in 2005/2006, occurred some days before the changes in the zonal circulation in the stratosphere, indicating a downward propagation of the circulation disturbances from the mesosphere-lower thermosphere (MLT) region to the stratosphere during the SSW events. Mbatha et al. (2010) observed a similar reversal of the mean zonal wind at the MLT approximately 7 days before the reversal at 10 hPa, during the Southern SSW in September 2002.

Although the strong stratospheric–mesospheric coupling during these extreme winter events has been recognised and extensively studied, only a small number of studies investigated the low-latitude stratospheric–mesospheric system response to SSWs. Pancheva et al. (2008) performed a study on the latitudinal wave coupling of the stratosphere and mesosphere during the major SSW in 2003/2004, and found an inverse relationship between the variability of the zonal mean flows at the high and low-latitude stratosphere related to the SSW. They found that this inverse relationship is produced by global-scale zonally symmetric waves (PWs with zonal wave number 0) with periods of ~ 22 – 23 , ~ 16 and ~ 11 days. Sathishkumar et al. (2009) investigated the dynamical response of the low-latitude middle atmosphere to major SSWs by a comparison of the zonal mean temperature and zonal winds at 8.75°N and 60°N for the winters 1995–1996 (no SSW), 1998–1999, 2003–2004, 2005–2006 (SSW winters), and found a change of wind direction from E-ward to W-ward at 8.75°N several days before the onset of the SSWs. These winds then slowly decelerated and reversed to weak E-ward winds again, which then persisted during the SSW events.

This study discusses the response in Seoul, S. Korea [37.3°N , 126.3°E] to the warming events in January–February 2008. The paper is organised as follows: In Section 2 we will describe the different datasets used. Section 3 provides an overview of the most important characteristics of the SSWs in January and February 2008 while the observations obtained in Seoul are presented and analysed in Section 4.

2. Data

Temperature, wind and potential vorticity data were provided by the European Centre for Medium-Range Weather Forecasts (ECMWF). The ECMWF T799L91 reanalyses data used here, is processed on a $1.125^\circ \times 1.125^\circ$ latitude–longitude grid, between 1000 and 0.01 hPa, and with a 6 h time resolution (0, 6, 12 and 18 UTC). Information and publications on the ECMWF analysis data are available at <http://www.ecmwf.int/publications/>.

Direct measurements of temperature and H_2O profiles were taken from the Microwave Limb Sounder (MLS) onboard the Aura satellite (Waters et al., 2006). MLS measures the microwave thermal emission from the Earth's limb and delivers vertical profiles from the upper tropo-

sphere up to the mesosphere for a range of gas phase atmospheric species, temperature and cloud ice density. The v2.2 H_2O data product is available between 316 and 0.001 hPa, with a single-profile precision of ~ 0.2 – 0.3 ppmv (4%–9%), and a vertical resolution of ~ 3 – 4 km in the stratosphere. The precision and vertical resolution deteriorate with increasing height above the stratopause. Over the pressure range 0.1–0.01 hPa the precision degrades from 0.4 to 1.1 ppmv (6%–34%), and the vertical resolution degrades to ~ 12 – 16 km (Lambert et al., 2007). Aura MLS temperature profiles have a precision of 1 K or better from 316 hPa to 3.16 hPa, degrading to ~ 3 K at 0.001 hPa. The vertical resolution is 3 km at 31.6 hPa, degrading to 6 km at 316 hPa and to ~ 13 km at 0.001 hPa (Schwartz et al., 2008).

The Seoul Water vapour RAdiometer (SWARA) is a GBMW radiometer and has been operational in Seoul since November 2006. It is a joint project of the University of Bern, Switzerland, and the Sookmyung Women's University of Seoul, S. Korea. SWARA measures the 22 GHz emission line of H_2O and delivers profiles between 1 and 0.01 hPa. Its time resolution varies from hours in winter up to weeks during summer. SWARA data has a precision of 7% at 1 hPa, decreasing to 14% at 0.1 hPa and 17% at 0.03 hPa. A detailed description of the calibration, retrieval and validation with Aura MLS is given by De Wachter et al. (2011). The validation study shows differences between SWARA and Aura MLS of better than 2% between 1 and 0.2 hPa, then declining nearly linearly to $\sim 14.5\%$ between 0.2 and 0.01 hPa.

Complementary to the Korean-stationed H_2O radiometer, the University of Bern has been operating the Middle Atmospheric Water vapour RAdiometer (MIAWARA) in Bern [46.9°N , 7.5°E] since 2002 (Deuber et al., 2004). MIAWARA is operated as an NDACC (Network for the Detection of Atmospheric Composition Change) instrument, and delivers middle atmospheric H_2O profiles between 10 and 0.01 hPa as well as tropospheric profiles (Haeefe and Kämpfer, 2010). A detailed intercomparison of five 22 GHz ground-based instruments, including SWARA and MIAWARA, was performed by Haeefe et al. (2009).

3. Characteristics of the SSWs in January–February 2008

An overview of the stratospheric conditions in the Northern Hemisphere, from January to March 2008, is given by the ECMWF temperature, wind and potential vorticity data, presented in Figs. 1 and 2.

Fig. 1 shows the latitude-time cross sections of the zonal means of temperature and zonal wind at 10 hPa (~ 32 km), and of the zonal and meridional wind at 1 hPa (~ 48 km). The latitude-circle of Bern (47°N) and Seoul (37°N) are marked by the black horizontal lines.

The beginning of 2008 was characterized by four SSW events (Fig. 1 (a)); three minor SSWs during late January, early February and (less pronounced) in mid February, and

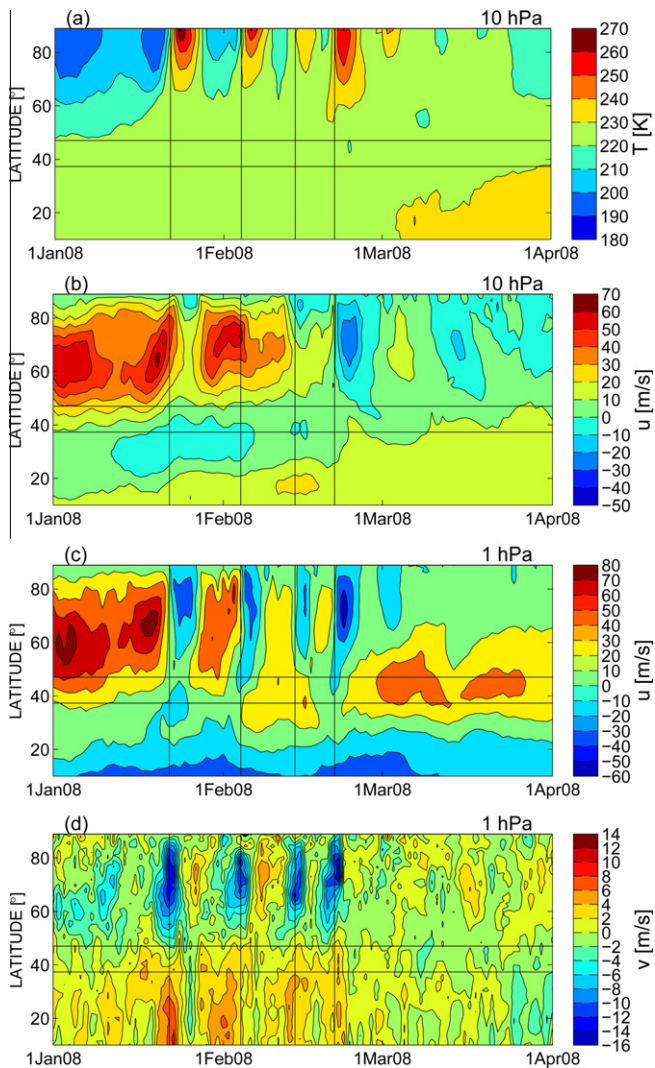


Fig. 1. Latitude–time cross section between 10°N and 89°N of ECMWF zonal mean of: (a) temperature at 10 hPa, (b) zonal wind at 10 hPa, (c) zonal wind at 1 hPa, and (d) meridional wind at 1 hPa. The horizontal black lines mark the 37°N and 47°N latitude-circles of Seoul and Bern. The onsets of the minor and major SSWs are indicated by the black vertical lines.

a major warming from 21 to 28 February, as also reported by Flury et al. (2009), Wang and Alexander (2009) and Alexander and Shepherd (2010).

The zonal wind at 10 hPa (Fig. 1 (b)) clearly visualizes the strong E-ward winter jet at high latitudes in January and February, with velocities up to 70 m/s, and the reversal of these E-ward winds during the major SSW. At lower latitudes, a reversal of the weak E-ward wind at 20°–45°N was recorded from 12 January to 6 February. In addition, one can see a strengthening of the weak E-ward wind after the onset of the major SSW.

At 1 hPa (Fig. 1 (c)), a reversal of the zonal wind is clearly visible for latitudes $> 50^\circ\text{N}$ during all (minor and major) SSWs. At latitudes between 30° and 45°N, the weak E-ward flow reverses only during the first SSW. One can see a strengthening of the E-ward flow in mid February for the duration of 2 weeks, and a second increase after the onset

of the major SSW. Pancheva et al. (2008) found an inverse relation between the zonal mean flow reversal at high latitudes and the strengthening of the E-ward zonal mean flow at low-latitudes at 1 hPa for the major SSW in 2003–2004. The same behaviour is noted here during the major warming, with the exception that the strengthening of the E-ward low-latitude winds starts a few days later than the onset of the high-latitude wind reversal from E-ward to W-ward.

For the meridional winds at 1 hPa (Fig. 1 (d)), a noteworthy wind flow is evident with strong S-ward motion for latitudes $> 50^\circ\text{N}$ and strong(er) N-ward motion at low-latitudes during the SSWs. Note that the strong S-ward flow at high latitudes starts several days before the SSWs with maxima at the onset of the SSW. To the Author's knowledge there are currently no studies that have reported the detection of similar meridional flow patterns at stratopause level. The majority of reports on meridional wind observations during SSWs are from localised MLT meridional wind measurements by MF and HF radars.

The SSWs of January–February 2008 are polar vortex displacement events. Fig. 2 shows ECMWF potential vorticity (PV) maps at the 600 K and 850 K isentropes (~ 25 hPa and ~ 10 hPa) for 11, 21 and 28 February 2008 (top to bottom). The locations of Bern and Seoul are indicated by the white dots. A clear displacement of the polar vortex towards central Europe is observed, with a simultaneous weakening of the vortex. At 850 K the vortex had dispersed by 28 February into a spiral-structured filament.

Flury et al. (2009) performed a detailed study of the response at mid latitudes to the major SSW, when the polar vortex shifted over Bern on 19 February. Investigation of the TIMED/SABER data showed a clear stratospheric warming over Bern accompanied by a cooling in the lower stratosphere and mesosphere. Simultaneously, a depletion in stratospheric O_3 and an enhancement of stratospheric and mesospheric H_2O were captured by the ground-based observations in Bern. Goncharenko and Zhang (2008) investigated the response of the warming events in January 2008 in the ion temperature from observations obtained by the Millstone Hill incoherent scatter radar ($42.6^\circ\text{N}, 228.5^\circ\text{E}$). They identified alternating regions of warming in the lower thermosphere and cooling above 150 km altitude, suggestive of a strong coupling from the lower atmosphere to the ionosphere during the (minor) warming events.

This section gave an overview of the overall characteristics of the SSWs in January–February 2008. Observations of the effects of SSWs at low-latitudes are sparse; the following section therefore outlines the response to the SSW events at the low-latitude station in Seoul, S. Korea.

4. Observations in Seoul [37.3°N, 126.3°E] in January–February 2008

Fig. 3 shows the Aura MLS temperature profiles in Seoul between 30 and 0.001 hPa for the same time period as Fig. 1. The Aura MLS profiles are selected within

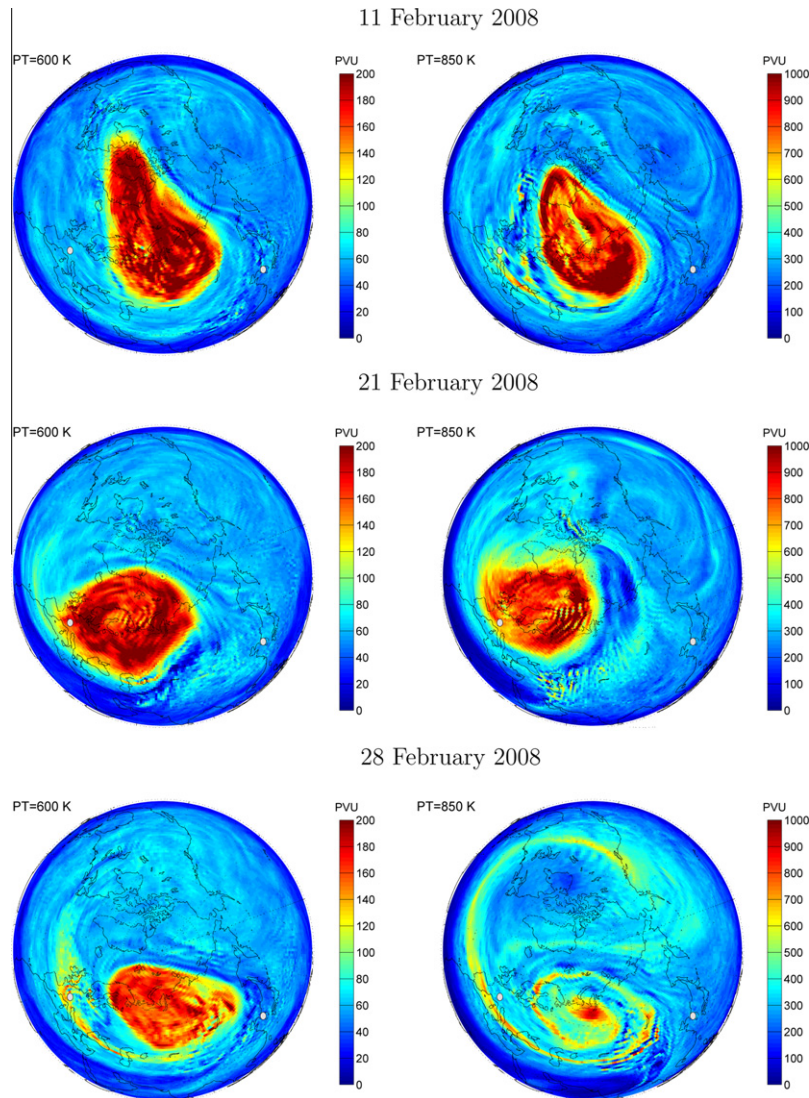


Fig. 2. ECMWF Potential Vorticity [PVU] maps at the (left) 600 K (~ 25 hPa) and (right) 850 K isentropic level (~ 10 hPa) for 11, 21 and 28 February 2008. The white dots pinpoint Bern and Seoul.

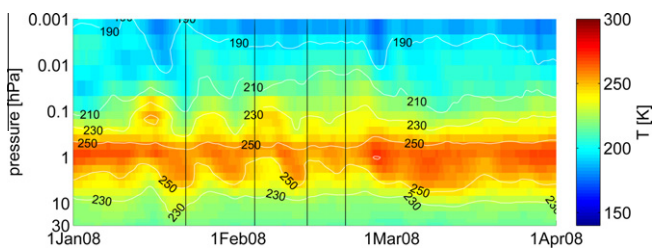


Fig. 3. Aura MLS temperatures over Seoul between 30 and 0.001 hPa, for January–March 2008. The vertical lines indicate the onset of the SSWs, as in Fig. 1.

± 200 km in latitude and ± 400 km in longitude from the observation site. A mesospheric cooling of ~ 10 – 20 K for pressures ≤ 0.01 hPa was recorded during mid-January, before the onset of the first minor warming, and at the end of the major SSW. Very pronounced are the strong oscillations between 10 and 0.05 hPa, from 11 January to

21 February (start of the major SSW). A wavelet-like analysis was applied to these timeseries, which followed the analysis described in Hocke (2009). In brief, first the temperature data is interpolated to a regular grid with a 6 h resolution. Then a bandpass-filtering is applied for periods between 0.6 to 20 days, with a varying stepsize ranging from 0.05 to 0.2 days. The amplitude of a period is correspondingly derived from the running average (integral) computed for the absolute values of the bandpass-filtered series, multiplied by $\pi/2$. The results for the Aura MLS temperature at 0.15 hPa is given in the left plot of Fig. 4, and shows a clear peak in amplitude of 10 K for a period ~ 10 – 14 days. These signatures of PW activity start in January and cease at the onset of the major SSW.

Following the aforementioned wavelet-like analysis, the periodicities in the mesospheric H_2O data at 0.19 hPa were investigated. Peak amplitudes of 0.45 ppmv were found for periods ~ 6 – 10 days during the major SSW and are

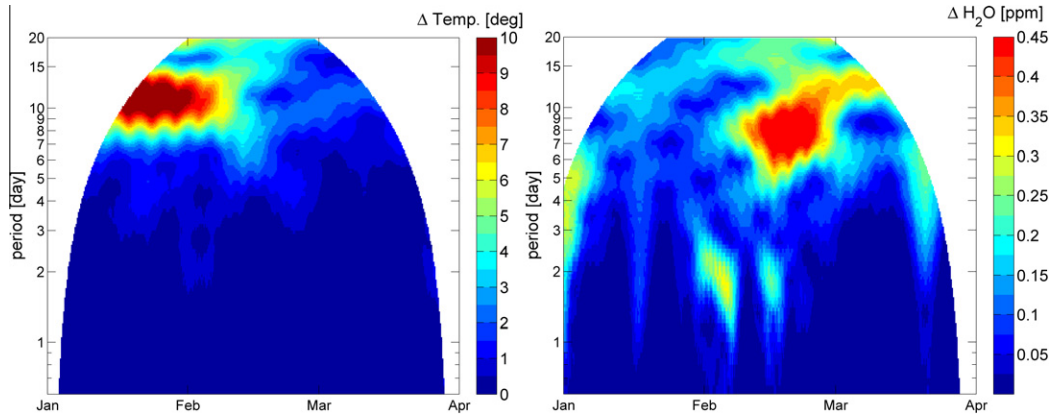


Fig. 4. Dynamic amplitude spectra, between January and April 2008, of [left] Aura MLS temperature over Seoul at 0.15 hPa, and of [right] SWARA H₂O VMR at 0.19 hPa.

displayed in the right plot of Fig. 4. The same periods were observed in the Aura MLS H₂O data, with an amplitude of ~0.35 ppmv (not shown here). Hence, indication of PW activity is found in the mesospheric H₂O at low latitudes during the major SSW, although it is difficult to be conclusive about these results. Coinciding H₂O oscillations with periods ~10–14 days are not found during the time of the observed temperature oscillation. The strong temperature oscillation belongs to the alternating pattern of warming and cooling around the stratopause (Fig. 3). If the temperature oscillation is caused by adiabatic expansion and compression it is clear that the volume mixing ratio (VMR) of H₂O cannot show a coincident oscillation.

Fig. 5 (a) shows the timeseries of H₂O at 0.1 hPa observed by SWARA in Seoul. Simultaneously, the H₂O distribution at 0.1 hPa observed by MIAWARA in Bern is shown in black. To validate these results, the Aura MLS H₂O observations for the two locations are given in grey in Fig. 5 (b). Here the Aura MLS data is taken according to the same criteria mentioned above for the temperature profiles, and the Aura MLS data is convolved with the averaging kernels of the ground-based instruments to account for the differing resolution between the satellite and ground-based data. There is a good agreement between the observations, with only a small bias for the Seoul data. However, the same overall variations in H₂O are captured by the satellite and ground-based instruments.

Returning to Fig. 5 (a), there exists a clear anticorrelation in the mesospheric H₂O observations, which is suggestive of a wave one-like pattern. From the Seoul measurements a decrease of ~3 ppmv (~40%) is observed in February 2008, reaching a minimum during the major SSW. In Bern, an increase of ~1.5 ppmv is observed, as previously reported by Flury et al. (2009). In Fig. 5 (b), overlaid in blue is the ECMWF PV at 10 hPa. We see a clear correlation between H₂O VMR and PV over Bern during the major warming. Also during the first 2 minor warmings, PV values are enhanced over Bern. As can be

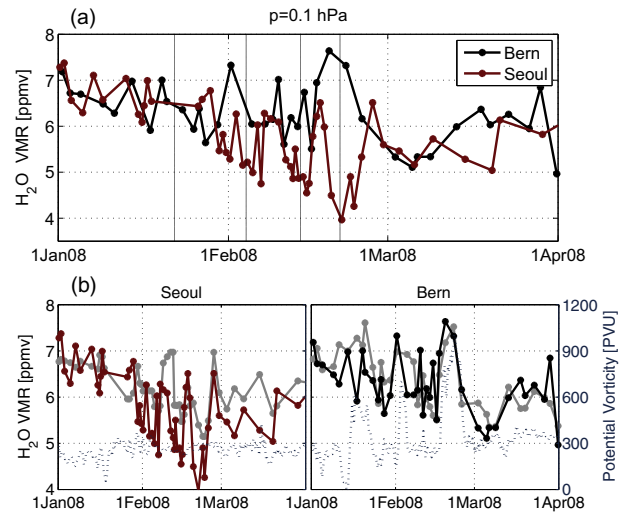


Fig. 5. (a) H₂O volume mixing ratio [ppmv] at 0.1 hPa, observed by the GBMW radiometers in Bern (black) and Seoul (red). (b) Timeseries of Aura MLS H₂O (grey) at 0.1 hPa at Seoul [left] and Bern [right] compared to the ground-based H₂O observations (red and black resp). Aura MLS data is convolved with the averaging kernels of the ground-based instruments. ECMWF potential vorticity values [in PVU] at 10 hPa are given for both sites by the blue dashed line [right y axis], corresponding to the 850 K isentropic level maps shown in Fig. 2. (For interpretation of the references to colour in this figure legend, the reader is referred to the web version of this article.)

seen from the PV maps shown in Fig. 2, PV values over Seoul are hardly varying.

A trajectory analysis was conducted to explain the origin of these air masses. Herewith, the TomTom model (Flury et al., 2008) was used, a trajectory model developed at the University of Bern, which interpolates ECMWF wind data on the air parcel location. Under the assumption of isentropic motion, the air mass is traced with a time resolution of 1 h.

Fig. 6 shows the backward trajectories, calculated at the 3200 K isentropic (~0.1 hPa), arriving at Seoul and at ECMWF grid points in a 1.125° square around Seoul, for different days in February 2008, at midnight ±12 h,

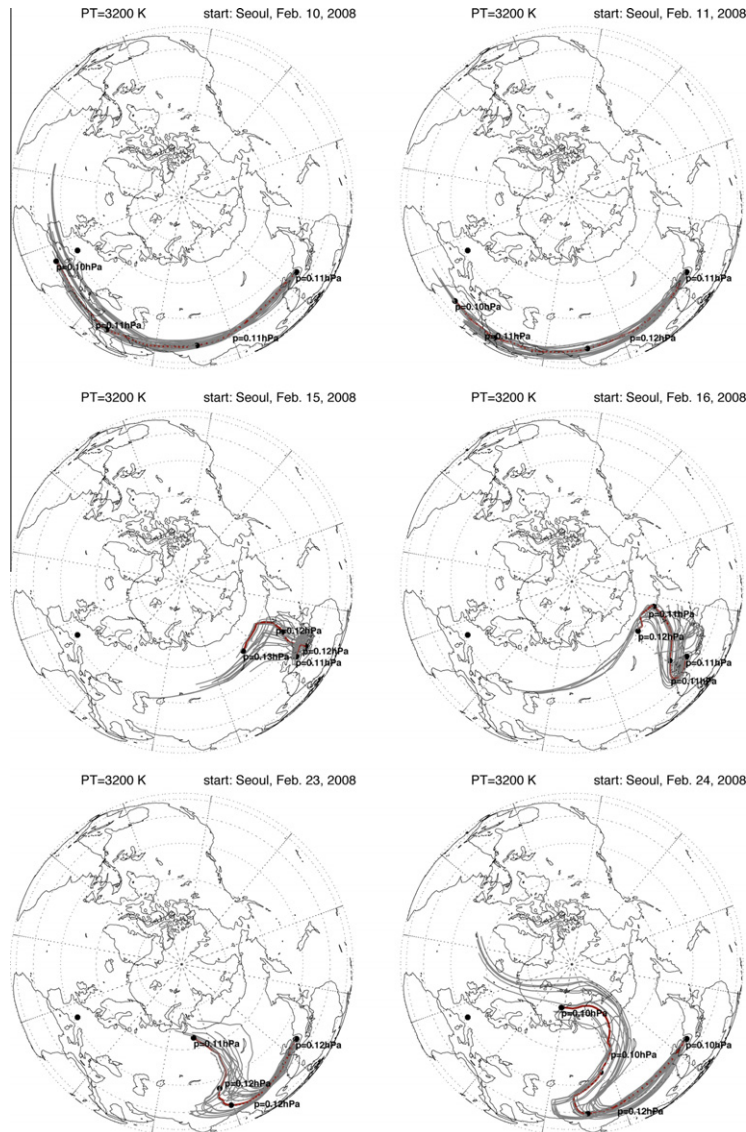


Fig. 6. Three-day backward trajectories arriving at Seoul and at locations in a 1.125° grid around Seoul, calculated on the 3200 K [~ 0.1 hPa] isentrope by the TomTom model, for different days ± 12 h, every 6 h. Here the different runs are shown for 10 and 11 February 2008 [top], 15 and 16 February 2008 [middle], and 23 and 24 February 2008 [bottom]. The red line corresponds to the trajectory arriving at midnight at Seoul. The black dots are placed at 24 h-intervals and label the pressure level. (For interpretation of the references to colour in this figure legend, the reader is referred to the web version of this article.)

every 6 h. The grey trajectories correspond to the different location and time offsets, the red line corresponds to the trajectory arriving at midnight at Seoul.

From the two top figures it is visible that the air mass follows the E-ward jet on 10 and 11 February (no SSW), as one would assume. Backward trajectories calculated during the major SSW and the subsequent H_2O decrease (15–16 and 23–24 February) are of polar origin (Fig. 6, middle and bottom). This indicates a meridional transport of H_2O -poor air from the polar region to Seoul during the polar vortex displacement, explaining the sudden decrease of H_2O VMR observed by SWARA at Seoul (Fig. 5).

In contrast, for 19 and 20 February (not shown here), the trajectories follow the E-ward jet, corresponding to

when an increase in H_2O VMR is observed to nominal values of ~ 6 ppmv, as shown in Fig. 5.

Flury et al. (2009) performed trajectory analysis to explain the increase in H_2O at Bern and found that the air was of subtropical origin where the H_2O VMR was greater than over Bern.

5. Conclusion

SSW are dynamic phenomena with a strong coupling between the stratosphere and (lower) mesosphere. This study captured the overall characteristics of the SSWs during the winter of January–February 2008, and the response to these warmings in Seoul, S. Korea, where PW activity with a period ~ 10 –14 days was observed in

the mesospheric temperature prior to the major warming in mid February 2008, and periodic oscillations with a period ~6–10 days were found in the mesospheric H₂O data during the major SSW. A decrease in mesospheric H₂O of ~40% was observed in Seoul during the major warming, while an H₂O enhancement was observed in Bern. Trajectory analysis showed that during the major SSW, when the polar vortex shifted towards central Europe, polar mesospheric air was brought to Seoul, while the enhanced H₂O air arriving at Bern was of subtropical origin. These signatures indicate strong coupling between the dynamic regimes of the low- and high-latitudes regions during boreal SSW events.

Acknowledgements

The Authors would like to thank SKORE-A for supporting this project in addition to funds by the Swiss National Science Foundation under Grant No. 200020_124387, as well as the EC project GEOMon.

References

- Alexander, S.P., Shepherd, M.G. Lower stratospheric planetary wave activity. *Atmos. Chem. Phys.* 10, 707–718, 2010.
- Deuber, B., Kämpfer, N., Feist, D.G. A new 22-GHz radiometer for middle atmospheric water vapour profile measurements. *IEEE Trans. Geosci. Remote Sens.* 42 (5), 974–984, 2004.
- De Wachter, E., Haefele, A., Kämpfer, N., Ka, S., Lee, J.E., Oh, J.J. The Seoul water vapour radiometer for the middle atmosphere: calibration, retrieval and validation. *IEEE Trans. Geosci. Remote Sens.* 49, 1052–1062, 2011.
- Flury, T., Müller, S.C., Hocke, K., Kämpfer, N. Water vapor transport in the lower mesosphere of the subtropics: a trajectory analysis. *Atmos. Chem. Phys.* 8, 7273–7280, 2008.
- Flury, T., Hocke, K., Haefele, A., Kämpfer, N., Lehmann, R. Ozone depletion, water vapor increase, and PSC generation at midlatitudes by the 2008 major stratospheric warming. *J. Geophys. Res.* 114, D18302, doi:10.1029/2009JD011940, 2009.
- Garcia, R., Boville, B. Downward Control of the mean meridional circulation and temperature distribution of the polar winter stratosphere. *J. Atmos. Sci.* 51, 2238–2245, 1994.
- Goncharenko, L., Zhang, S.-R. Ionospheric signatures of sudden stratospheric warming: Ion temperature at middle latitude. *Geophys. Res. Lett.* 35, L21103, doi:10.1029/2008GL035684, 2008.
- Haefele, A., De Wachter, E., Hocke, K., Kämpfer, N., Nedoluha, G.E., Gomez, R.M., Eriksson, P., Forkman, P., Lambert, A., Schwarz, M. Validation of ground based microwave radiometers at 22 GHz for stratospheric and mesospheric water vapor. *J. Geophys. Res.* 114, D23305, doi:10.1029/2009JD011997, 2009.
- Haefele, A., Kämpfer, N. Tropospheric water vapor profiles retrieved from pressure broadened emission spectra at 22 GHz. *J. Atmos. Ocean. Technol.* 27, 167–172, doi:10.1175/2009JTECHA1334.1, 2010.
- Hocke, K. QBO in solar wind speed and its relation to ENSO. *J. Atmos. Solar-Terrest. Phys.* 71, 216–220, doi:10.1016/j.jastp.2008.11.017, 2009.
- Hoffman, P., Singer, W., Keuer, D., Hocking, W.K., Kunze, M., Murayama, Y. Latitudinal and longitudinal variability of mesospheric winds and temperatures during stratospheric warming events. *J. Atmos. Solar-Terrest. Phys.* 69, 2355–2366, doi:10.1016/j.jastp.2007.06.010, 2007.
- Lambert, A., Read, W.G., Livesey, N.J., Santee, M.L., Manney, G.L., Froidevaux, L., Wu, D.L., Schwartz, M.J., Pumphrey, H.C., Jimenez, C., Nedoluha, G.E., R.E. Cofield, D.T., Cuddy, W.H., Daffer, B.J., Drouin, R.A., Fuller, R.F., Jarnot, Knosp, B.W., Pickett, H.M., Perun, V.S., Snyder, W.V., Stek, P.C., Thurstans, R.P., Wagner, P.A., Waters, J.W., Jucks, K.W., Toon, G.C., Stachnik, R.A., Bernath, P.F., Boone, C.D., Walker, K.A., Urban, J., Murtagh, D., Elkins, J.W., E. Atlas, E. Validation of the Aura Microwave Limb Sounder middle atmosphere water vapor and nitrous oxide measurements. *J. Geophys. Res.* 112, D24S36, doi:10.1029/2007JD008724, 2007.
- Liu, H.-L., Roble, R.G. A study of a self-generated stratospheric sudden warming and its mesospheric-lower thermospheric impacts using the coupled TIME-GCM/CCM3. *J. Geophys. Res.* 107 (D23), 4395, doi:10.1029/2001JD001533, 2002.
- Matsuno, T. A dynamical model of the stratospheric sudden warming. *J. Atmos. Sci.* 28, 1479–1494, 1971.
- Mbatha, N., Sivakumar, V., Malinga, S.B., Bencherif, H., Pillay, S.R. Study on the impact of sudden stratosphere warming in the upper mesosphere-lower thermosphere regions using satellite and HF radar measurements. *Atmos. Chem. Phys.* 10, 3397–3404, 2010.
- Pancheva, D., Mukhtarov, P., Mitchell, N.J., Andonov, B., Merzlyakov, E., Singer, W., Murayama, Y., Kawamura, S., Xiong, J., Wan, W., Hocking, W., Fritts, D., Riggan, D., Meek, C., Manson, A. Latitudinal wave coupling of the stratosphere and mesosphere during the major stratospheric warming in 2003/2004. *Ann. Geophys.* 26, 467–483, 2008.
- Sathishkumar, S., Sridharana, S., Jacobi, Ch. Dynamical response of low-latitude middle atmosphere to major sudden stratospheric warming events. *J. Atmos. Solar-Terrest. Phys.* 71, 857–865, doi:10.1016/j.jastp.2009.01.002, 2009.
- Schwartz, M.J., Lambert, A., Manney, G.L., Read, W.G., Livesey, N.J., Froidevaux, L., Ao, C.O., Bernath, P.F., Boone, C.D., Cofield, R.E., Daffer, W.H., Drouin, B.J., Fetzer, E.J., Fuller, R.A., Jarnot, R.F., Jiang, J.H., Jiang, Y.B., Knosp, B.W., Krüger, K., Li, J.-L.F., Mlynarczyk, M.G., Pawson, S., Russell III, J.M., Santee, M.L., Snyder, W.V., Stek, P.C., Thurstans, R.P., Tompkins, A.M., Wagner, P.A., Walker, K.A., Waters, J.M., Wu, D.L. Validation of the Aura Microwave Limb Sounder temperature and geopotential height measurements. *Geophys. Res. Letters* 113, D15S11, doi:10.1029/2007JD008783, 2008.
- Siskind, D.E., Coy, L. Observations of stratospheric warmings and mesospheric coolings by the TIMES SABER instrument. *Geophys. Res. Letters* 32, L09801, doi:10.1029/2005GL022399, 2005.
- Siskind, D.E., Eckermann, S.D., McCormack, J.P., Larry Coy, L., Hoppel, K.W., Baker, N.L. Case studies of the mesospheric response to recent minor, major and extended stratospheric warmings. *J. Geophys. Res.* 115, D00N03, doi:10.1029/2010JD014114, 2010.
- Walterscheid, R.L., Sivjee, G.G., Roble, R.G. Mesospheric and lower thermospheric manifestations of a stratospheric warming event over Eureka, Canada (80°N). *Geophys. Res. Lett.* 27 (18), 2897–2900, 2000.
- Wang, L., Alexander, M.J. Gravity wave activity during stratospheric sudden warmings in the 2007/2008 Northern Hemisphere winter. *J. Geophys. Res.* 114, D18108, doi:10.1029/2009JD011867, 2009.
- Waters, J.W., Froidevaux, L., Harwood, R.S., Jarnot, R.F., Pickett, H.M., Read, W.G., Siegel, P.H., Cofield, R.E., Filipiak, M.J., Flower, D.A., Holden, J.R., Lau, G.K., Livesey, N.J., Manney, G.L., Pumphrey, H.C., Santee, M.L., Wu, D.L., Cuddy, D.T., Lay, R.R., Loo, M.S., Perun, V.S., Schwartz, M.J., Stek, P.C., Thurstans, R.P., Boyles, M.A., Chandra, S., Chavez, M.C., Chen, G.-S., Chudasama, B.V., Dodge, R., Fuller, R.A., Girard, M.A., Jiang, J.H., Jiang, Y., Knosp, B.W., LaBelle, R.C., Lam, J.C., Lee, K.A., Miller, D., Oswald, J.E., Patel, N.C., Pukala, D.M., Quintero, O., Scaff, D.M., Snyder, W.V., Tope, M.C., Wagner, P.A., Walch, M.J. The Earth Observing System Microwave Limb Sounder (EOS MLS) on the Aura satellite. *IEEE Trans. Geosci. and Remote Sensing* 44 (5), 1075–1092, 2006.